Title
A mass-balance/photochemical assessment of DMS sea-to-air flux as inferred from NASA GTE PEM-West a and B observations

Journal
Journal of Geophysical Research Atmospheres, 104(D5)

ISSN
0148-0227

Authors
Chen, G
Davis, D
Kasibhatla, P
et al.

Publication Date
1999-03-20

DOI
10.1029/1998JD100039

JOURNAL OF GEOPHYSICAL RESEARCH, VOL. 104, NO. D5, PAGES 5471-5482, MARCH 20, 1999

A mass-balance/photochemical assessment of DMS sea-to-air flux as inferred from NASA GTE PEM-West A and B observations

G. Chen,[1] D. Davis,[1] P. Kasibhatla,[2] A. Bandy,[3] D. Thornton,[3] and D. Blake[4]

Abstract. This study reports dimethyl sulfide (DMS) sea-to-air fluxes derived from a mass-balance/photochemical-modeling approach. The region investigated was the western North Pacific covering the latitude range of 0°-30°N. Two NASA airborne databases were used in this study: PEM-West A in September-October 1991 and PEM-West B in February-March 1994. A total of 35 boundary layer (BL) sampling runs were recorded between the two programs. However, after filtering these data for pollution impacts and DMS lifetime considerations, this total was reduced to 13. Input for each analysis consisted of atmospheric DMS measurements, the equivalent mixing depth (EMD) for DMS, and model estimated values for OH and NO_3. The evaluation of the EMD took into account both DMS within the BL as well as that transported into the overlying atmospheric buffer layer (BuL). DMS fluxes ranged from 0.6 to 3.0 μmol m^{-2} d^{-1} for PEM-West A (10 sample runs) and 1.4 to 1.9 μmol m^{-2} d^{-1} for PEM-West B (3 sample runs). Sensitivity analyses showed that the photochemically evaluated DMS flux was most influenced by the DMS vertical profile and the diel profile for OH. A propagation of error analysis revealed that the uncertainty associated with individual flux determinations ranged from a factor of 1.3 to 1.5. Also assessed were potential systematic errors. The first of these relates to our noninclusion of large-scale mean vertical motion as it might appear in the form of atmospheric subsidence or as a convergence. Our estimates here would place this error in the range of 0 to 30%. By far the largest systematic error is that associated with stochastic events (e.g., those involving major changes in cloud coverage). In the latter case, sensitivity tests suggested that the error could be as high as a factor of 2. With improvements in such areas as BL sampling time, direct observations of OH, improved DMS vertical profiling, direct assessment of vertical velocity in the field, and preflight (24 hours) detailed meteorological data, it appears that the uncertainty in this approach could be reduced to ± 25%.

1. Introduction

Dimethyl sulfide (DMS) is known to be a by-product of biological processes involving marine phytoplankton [*Barnard et al.*, 1982; *Dacey and Wakeham*, 1986; *Keller et al.*, 1989]. Emissions of DMS have been estimated to be around 60% of the total natural sulfur gas released to the atmosphere [e.g., *Andreae and Raemdonck*, 1983; *Bates et al.*, 1992; *Berresheim et al.*, 1995]. In clean background marine boundary layer (BL) air, DMS is oxidized mainly by OH and, to a much lesser extent, NO_3. Chamber type studies have shown that the oxidation of DMS in the troposphere (via OH) can produce SO_2, methane sulfonic acid (MSA), dimethyl sulfoxide (DMSO), dimethyl sulfone ($DMSO_2$) plus other minor products [*Barnes et al.*, 1989, 1993, 1994; *Sørensen et al.*, 1996; *Berresheim et al.*, 1995, and references therein]. Detailed kinetic investigations of the DMS/OH reaction have also shown that this reaction proceeds by two independent channels: abstraction and addition [*Hynes et al.*, 1986]. The SO_2 species now appears to be a product of both the addition and abstraction channels [*Barnes et al.*, 1993; *Sørensen et al.*, 1996; *Davis et al.*, 1998a, b]. In the atmosphere SO_2 is oxidized to H_2SO_4, leading to either aerosol growth or to the formation of new sulfate particles [e.g., *Kreidenweis and Seinfeld*, 1988; *Berresheim et al.*, 1995, and references therein]. Since these aerosol particles, in turn, have the potential for impacting upon the Earth's climate, both from direct as well as indirect processes [*International Geosphere-Biosphere Programme (IGBP)*, 1988; *International Global Atmospheric Chemistry (IGAC)*, 1994; *Intergovernmental Panel on Climate Change (IPCC)*, 1995], the linkage between DMS and aerosols is considered an important component of the planetary climate system [*IPCC*, 1995].

In general, two different approaches have been used to determine the amount of DMS released from the ocean to the

[1]School of Earth and Atmospheric Sciences, Georgia Institute of Technology, Atlanta.
[2]School of Environment, Duke University, Durham, North Carolina.
[3]Department of Chemistry, Drexel University, Philadelphia, Pennsylvania.
[4]Department of Chemistry, University of California, Irvine.

Paper number 1998JD100039.
0148-0227/99/1998JD100039$09.00

atmosphere. One of these has focused on DMS sea-water measurements; the other has used only atmospheric observations of DMS. In the first approach, the DMS flux is assumed to be simply the product of the surface sea-water DMS concentration and a sea-to-atmosphere transfer efficiency factor. The latter quantity has been given the name "piston velocity." In fact, the largest uncertainty in the air-sea exchange approach is now thought to lie in the evaluation of this transfer efficiency factor. In an effort to give this approach more general applicability, the piston velocity has also been parameterized as a function of wind speed and temperature. The most commonly used parameterizations are those developed by *Liss and Merlivat* [1986], *Wanninkhof et al.* [1985], and *Smethie et al.* [1985]. All are found to agree within a factor of 2 [*Jodwalis and Benner*, 1996]; however, this still does not preclude the possibility of yet unidentified systematic errors. The air-sea exchange approach has been widely used in estimating DMS fluxes, reflecting in no small part its simplicity, the availability of a large sea-water DMS database (accumulated over more than a decade), the availability of the GCMs (general circulation model) and wind field data [e.g., *Bates et al.*, 1987; *Erickson et al.*, 1990; *Langner and Rodhe*, 1991; *Spiro et al.*, 1992; *Penner et al.*, 1994; *Pham et al.*, 1995; *Chin et al.*, 1996].

As noted above, the alternative to sea-water-based flux estimates has been the use of atmospheric observations of DMS. For example, *Putaud and Nguyen* [1996] evaluated the DMS flux from the vertical gradient in the DMS mixing ratio (i.e., 1-20 m) in combination with eddy diffusion coefficients derived from meteorological observations. Using still a different approach, *Jodwalis and Benner* [1996] estimated the DMS flux using the variance and inertial-dissipation method. This approach was based upon an analysis of atmospheric DMS time series data. *Lenschow et al.* [1999] have also employed a mixed-layer/gradient method in which the DMS flux was determined from gas phase measurements of DMS at several different altitudes within the BL as well as at altitudes immediately above. The final flux estimating approach, based on atmospheric measurements of DMS, has been labeled here the mass-balance/photochemical-modeling methodology. Far more extensively used than the other approaches, based on gas phase measurements of DMS, this method recognizes that if DMS is destroyed by local photochemistry, and that photochemistry can be well characterized (e.g., clean background marine conditions), the DMS sea-to-air flux can be estimated from mass conservation considerations. It readily lends itself to a variety of platforms including ground-based, shipboard, and airborne [*Ayers et. al.*, 1995; *Davison and Hewitt*, 1992; *Thompson et al.*, 1990; *Thompson et al.*, 1993; *Saltzman and Cooper*, 1989; *Yvon et al.*, 1996; *Davis et al.*, 1990; *Davis et al.*, 1998b; G. Chen et al., A study of tropical DMS oxidation chemistry: Comparison of Christmas Island field observations of SO_2 and DMS with model simulations, submitted to *Journal of Atmospheric Chemistry*, 1999].

The current study uses the mass-balance/photochemical modeling approach in conjunction with data collected during NASA's airborne program Global Tropospheric Experiment/ Pacific Exploratory Mission-West (GTE PEM-West). This program had a region of study that encompassed the tropical and extratropical latitudes of the central and western North Pacific and covered a time period that ranged from the fall 1991 (PEM-West A) to winter 1994 (PEM-West B). DMS fluxes in this region of the Pacific have heretofore been based almost entirely upon sea-water DMS measurements. In most of these studies the piston velocity was estimated from climatologically averaged winds and sea-water temperatures. One of the more extensive of these sea-water measurement campaigns was that by *Bates et al.* [1987]. This study compiled over 1000 sea-water measurements for the North Pacific that covered both seasonal and regional DMS concentration trends in surface sea-water. These data were used to estimate the average DMS flux for six latitudinal bands spanning the range of 0°-80°N.

Still other studies that have examined the North Pacific have used GCM to estimate spatially resolved (latitude/longitude) global piston velocities [*Erickson et al.*, 1990; *Chin et al.*, 1996]. These values were then combined with *Bates et al.'s* [1987] summary DMS sea-water measurements. In *Erickson et al.'s* [1990] study, atmospheric DMS levels were simulated from the estimated fluxes and then compared to atmospheric DMS observations. They found reasonably good agreement with the observations for regions having low productivity while they disagreed (underestimated) with the levels for regions having the highest productivity. *Chin et al.* [1996] also estimated a global DMS flux field, again based upon GCM evaluated piston velocities and the marine data provided by Bates et al. These investigators then selected a DMS-SO_2 conversion efficiency factor that tended to simulate measured atmospheric nonsea-salt sulfate (NSS) levels as well as reasonable values for the ratio NSS-MSA. Their results were in reasonably good agreement with the NSS and NSS-MSA observations; however, they found that the resulting atmospheric levels of DMS were significantly higher than those reported from field studies. Thus these results could be interpreted to mean one of several things: that there is a missing atmospheric oxidizing source (e.g., higher levels of OH, NO_3, and/or halogen radicals), that nonbiogenic sources of sulfur are more effectively transported into the remote Pacific than currently thought, or that there is too high estimate of the DMS flux field in combination with a too low estimate for the DMS to SO_2 conversation.

We believe the mass-balance/photochemical-modeling approach has several important characteristics that make it worthwhile as an alternative way for evaluating global marine DMS fluxes. (1) It has the potential for looking at large geographical regions within a short time period when using an airborne sampling platforms; (2) it represents a totally independent method of assessing the DMS flux; and (3) with new airborne OH sensors now coming on-line, it offers the possibility in the near future of directly measuring nearly all critical parameters required to evaluate the DMS flux. Obviously, this approach might also provide further insight into the parameterization of the sea-water transfer-efficiency factor if common sampling sites were to be examined.

2. Approach and Model Description

2.1. Approach

For a well mixed boundary layer (BL), a commonly cited formulation for the DMS mass-balance is that shown in (1) [*Bandy et al.*, 1996; *Yvon et al.*, 1996; *Ayers et al.*, 1995; *Saltzman and Cooper*, 1989]:

$$\frac{d[DMS]}{dt} = \frac{F_{DMS}}{h} + \frac{W_e}{h}\left([DMS]_{BuL} - [DMS]_{BL}\right) - \left(k_{OH}[OH] + k_{NO_3}[NO_3]\right)[DMS] \quad (1)$$

In this equation the first term represents the oceanic source term, where F_{DMS} is the DMS sea-to-air flux and "h" is boundary layer height. The second term defines the loss of DMS due to photochemical oxidation by OH and NO_3, and the final term describes the DMS mass exchange between the BL and the zone immediately above which has recently been labeled the "buffer layer" (BuL) by *Russell et al.* [1998]. W_e in this formulation is the entrainment velocity and $[DMS]_{BuL}$ is the BuL DMS concentration. In fact, the practical application of (1) is most often limited by the quantitative evaluation of W_e [*Lenschow*, 1995]. This, in particular, can be a serious deficiency when the BL is not well capped. In this case, significant amounts of BL DMS can be vented into the BuL and thus represents a loss term for DMS. For PEM-West A and B, values for W_e could not be independently derived from in situ observations.

Equation (2) shows yet another frequently used mass-balance formulation for evaluating the DMS flux [e.g., *Thompson et al.*, 1993; *Davison and Hewitt,* 1992]. In this equation the exchange between the BL and BuL is neglected, and the DMS mass-balance consideration is based only on oceanic emissions and photochemical oxidation:

$$\frac{d[DMS]}{dt} = \frac{F_{DMS}}{h} - \left(k_{OH}[OH] + k_{NO_3}[NO_3]\right)[DMS] \quad (2)$$

In this case, "h" is defined as the mixed layer depth. Thus, when the BL is well capped, "h" is defined by the BL height. Given (2), if the DMS mixing ratio is known at an inflection point where $d[DMS]/dt = 0$ and the values of "h", [OH], and $[NO_3]$ can be evaluated independently, the DMS flux can be directly evaluated. Alternatively, F_{DMS} can be determined from a direct comparison of model and observed DMS profiles. In the latter case, the "best estimate" of F_{DMS} is determined by adjusting its value so as to minimize the difference between model calculated and observed DMS profiles.

The mixed layer depth used in past studies has typically been taken to be greater than 1 km. For example, *Thompson et al.* [1993] used 1.5 km, and *Yvon et al.* [1996] used 2.2 km. These values, however, are significantly higher than the typical marine boundary layer height of ~ 0.7 km [*Stull*, 1988]. Elevated values of "h" have primarily been used to deal with the problem of how to evaluate the flux associated with DMS that has mixed into the BuL or even the lower free troposphere [*Yvon et al.*, 1996]. The BuL is a zone in the lower troposphere that *Russell et al.* [1998] have recently described as defining a region of intermittent turbulence. It is a region into which significant quantities of DMS can frequently be mixed. This is particularly true when shallow convection is ongoing. The relative mass distribution of DMS between the BL and BuL depends upon both the intensity of BuL turbulence as well as the jump in stability in the transition from the BL to the BuL. If any degree of mixing does occur, the use of the more conventional marine BL height parameter "h" necessarily leads to an underestimate of the DMS flux. In fact, DMS levels in the BuL frequently do show significant vertical gradients, reflecting the intermittent nature of mixing in this region. This suggests that the most appropriate scale height to use should be lower than the top of the buffer layer but higher than the meteorological mixing depth (i.e., the BL height). Thus, under conditions where the rate of DMS oxidation is not too dissimilar for both the BuL and BL (which is a typical situation), the parameter "h" in (1) can be more appropriately replaced by what we have labeled the DMS equivalent mixing depth (EMD). This quantity is defined by (3):

$$EMD = \frac{1}{[DMS]_{BL}} \int [DMS](z)dz \quad (3)$$

The equivalent mixing depth can be viewed as the height of an atmospheric column that contains all DMS mass (both BuL and BL) but at BL concentrations. In principle, the value of EMD can be assessed from DMS airborne observations recorded during ascents and descents to and from the BL. From a practical point of view, however, the reliability of this assessment is found to be quite dependent upon the vertical resolution of the DMS measurements. An alternative in those cases where high-resolution DMS vertical profiles are not available is the use of a surrogate ocean source species such as CH_3I. The lifetime of CH_3I, controlled by UV photolysis, is typically a factor of 2 to 3 longer than that of DMS. Thus CH_3I can provide an upper-limit estimate of EMD. A lower-limit value for the EMD is that defined by the BL height itself. In the current study, because of the frequent absence of DMS data in both the BL and BuL, only upper- and lower-limit values could be assigned to the DMS flux.

2.2. Model Description

To assess the DMS flux, a modified mass conservation equation, (4), was employed in conjunction with the measured DMS and model generated diel profiles for OH and NO_3, e.g.,

$$\frac{d[DMS]}{dt} = \frac{F_{DMS}}{EMD} - \left(k_{OH}[OH] + k_{NO_3}[NO_3]\right)[DMS] \quad (4)$$

This equation is also based on the assumption that the large-scale mean vertical velocity for the region sampled approached zero. The photochemical box model employed to generate OH and NO_3 profiles was quite similar to that described previously by *Davis et al.* [1993, 1996a], *Chen* [1995], and *Crawford et al.* [1997, 1998]. This model contains 72 H_XO_Y - N_XO_Y - CH_4 gas kinetic/photochemical reactions and 146 non-methane hydrocarbon (NMHC) reactions, as well as 8 heterogeneous processes. The confidence level placed on the model generated OH profiles is based upon both intercompari-son with other photochemical models [*Davis et al.*, 1996a] as well as results from independent studies involving comparisons of modeled values of OH profiles with those directly measured in the field [R. L. Mauldin et al., OH measurement during PEM-Tropics: Observations versus model calculations, submitted to *J. Geophys. Res.*, 1998a; *Jefferson et al.*, 1998; *Davis et al.*, 1998b]. In the latter case, the level of agreement has ranged from 15 to 30%.

Concerning the nighttime oxidant NO_3, both reactions with DMS as well as deposition to aerosol surfaces were included. Thermal decomposition of NO_3 was not used due to a lack of supporting evidence [*Johnston et al.*, 1986; *H. F. Davis et al.*, 1993]. Sensitivity tests suggest that only in the case where the levels of NO_x were highly elevated did reaction with NO_3 represent a major loss channel for DMS. However, under clean marine background conditions, where NO_x levels have typically been found to be quite low (i.e. $\leq$ 10 pptv) [e.g., *McFarland et al.*, 1979; *Ridley et al.*, 1987; *Davis et al.*, 1987], oxidation of DMS by NO_3 is typically small when compared to OH oxidation (i.e., < 30%).

Input to our model consisted of median values for O_3, CO, H_2O, NO, NMHCs, temperature, and pressure. In this study, as in others, J values were adjusted to simulate actual solar/cloud conditions encountered in the field. However, since the typical boundary layer run lasted for less than 1 hour, an assessment of the solar history prior to the sampling was not possible. In lieu of this kind of information, cloud correction factors were evaluated for several general regions sampled during PEM-A and -B. In our case, the average cloud correction factors for PEM-A and -B were estimated at 0.9 and 0.85, respectively.

Under conditions where OH oxidation dominated DMS loss, the uncertainty in F_{DMS} was typically found to be most dependent on the "goodness" of the EMD evaluation and the extent to which the observed chemical snapshot of DMS (based on a single BL run) may have been recorded under conditions representative of solar conditions during the previous 24 hours. In fact, errors resulting from stochastic events, such as major changes in cloud coverage, are now considered to be the more important of the two. Sensitivity tests which explore the potential magnitude of this error are discussed in section 4.2.

The numerical method used to solve (4) was the quasi-steady-state approximation (QSSA) method developed by *Hesstvedt et al.* [1978]. Typically 4-10 days were required to reach a quasi-steady level for DMS. Values of F_{DMS} and EMD were normally kept constant over an entire diel cycle. The effects resulting from nonconstant EMD and F_{DMS} are discussed in section 4.2.

3. Observational Data

During PEM-West A and B, DMS measurements were recorded using the isotope dilution (ID)/gas chromatography (GC)/mass spectrometry (MS) technique [*Bandy et al.*, 1993]. Samples were cryogenically trapped for 3-4 min followed by GC separation and detection using a quadrapole mass spectrometer. Unique to the ID/GC/MS system was the routine injection of a calibration standard into each ambient DMS sample. The overall turnaround time for this analysis was typically 6-7 min. The limit of detection for DMS was given as 2-3 pptv [*Hoell et al.*, 1996]. Further details concerning the ID/GC/MS technique as well as the instrumentation used to measure other photochemical parameters are given by *Hoell et. al.* [1996, 1997].

A total of 35 BL DMS sampling runs were recorded during PEM-West A and B. For purposes of evaluating the DMS flux, however, only a subset of this total was found to be acceptable when using the mass-balance/photochemical-modeling approach. Two filters were employed to establish this suitability: (1) the chemical uniformity of the photochemical environment and (2) the DMS chemical lifetime. Regarding the first filter, only when the sampled environment reflected relatively clean marine background conditions was it considered acceptable. The argument here is that under conditions involving fluctuating pollution levels, both the relative as well as absolute magnitude of the DMS oxidation rates by OH and NO_3 would be highly uncertain over the 24-hour period preceding the actual sample collection time. In fact, continental outflow was present on several BL flight legs, particularly those recorded during PEM-B [*Crawford et al.*, 1998; *Merrill et al.*, 1997]. In all these cases the levels of most OH controlling species were found to be highly variable.

For purposes of defining the BL pollution problem, the following criteria were employed:

$$[NO_x] \geq 25 \text{ pptv}$$
$$[SO_2] \geq 85 \text{ pptv}$$
$$[CO] \geq 125 \text{ ppbv}$$

After filtering for pollution effects, 15 background marine BL runs remained, 12 from PEM-A and 3 from PEM-B. That fewer cases were found acceptable from PEM-B reflects the fact that during the February-March 1994 campaign much of the field sampling took place just off the coast of Asia. This is the time of year when significant releases of anthropogenic emissions flow from the Asian continent into the western North Pacific Ocean [*Crawford et al.*, 1998; *Merrill et al.*, 1997].

The second filter invoked in the current analysis of DMS fluxes involved the DMS chemical lifetime. For purposes of this analysis, only those DMS lifetimes $\leq$ 2.5 days were considered. This criteria was set forward in an attempt to ensure that only DMS released relatively near the sampling site was being considered in the flux determination. Thus this criterion was designed to minimize the uncertainty associated with long-range transport in the evaluation of the DMS flux. In the case of PEM-A and -B, application of the lifetime filter resulted in the removal of two additional runs from PEM-A, giving a final total of 13 runs evaluated. In Figure 1 we show the sampling locations of these 13 runs, and in Table 1 we summarize the median values of the photochemical parameters and DMS values used as input for our flux determinations.

As discussed in section 2.1, one of the critical factors requiring an independent evaluation when using (4) is the DMS equivalent mixing depth, EMD. However, during PEM-A and -B, the time resolution for DMS measurements was too low (i.e., ~ 6 min) to facilitate making the necessary vertical measurements of DMS to evaluate the EMD. Thus only lower and upper limits for the EMD were possible. These limiting values were based on independent assessments of the marine BL height and the EMD for CH_3I. Since the latter species has predominantly an oceanic source with a nominal lifetime of 3-6 days, it represents a good tracer for marine BL air [see, e.g., *Davis et al.*, 1996b; S. Liu et al., Tropospheric vertical transport over the tropical Pacific, submitted to *Journal of Geophysical Research*, 1997]. This species was typically measured with 1-2 min time resolution during the ascents and descents.

In the current study the value of the BL height, "h", as well as BuL height was derived from the high-resolution (10 s) vertical data recorded for several meteorological parameters. Of particular value were the potential temperature, θ, and the specific humidity, "q" [*Stull*, 1988]. As illustrative of how these parameters were used, Figure 2 shows both quantities plotted as a function of altitude. In this case, the top of the BL is defined as that altitude at which θ and "q" undergo a significant shift in value with increases in altitude, e.g., ~ 0.7 km, as indicated by a vertical long thin dash line. Similarly, the BuL height was estimated at ~ 1.8 km. Our "best estimate" of the BL height was typically defined from the average value calculated from four individual estimates involving θ and "q" values involving both the descent and ascent to/from the BL. The uncertainty assigned to this average was estimated from the maximum difference between the four independent values and the mean. Also shown in Figure 2 were the observed CH_3I vertical profile and estimated EMD. The latter quantity was

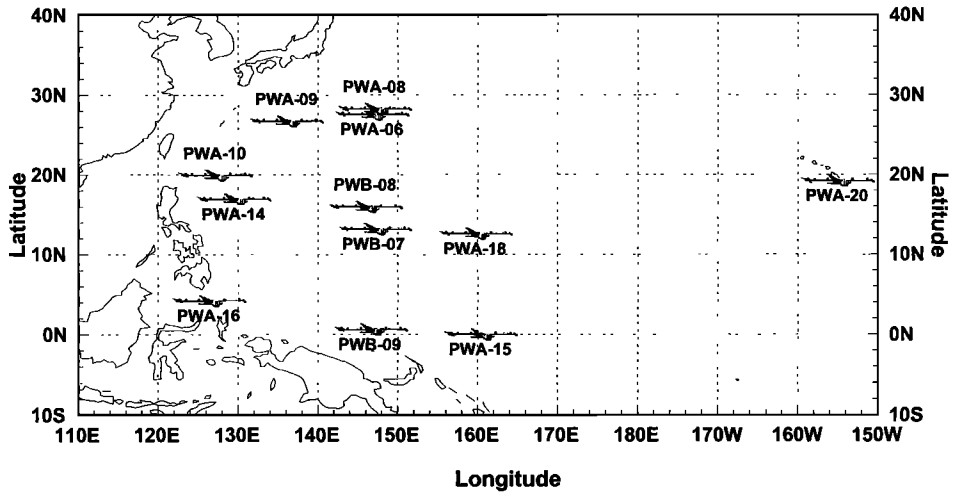

Figure 1. Geographical distribution of 13 BL runs selected for DMS flux analysis using the mass-balance/photochemical modeling approach. Aircraft symbols indicate sampling locations.

evaluated using the observed CH_3I profile and (3) with substitution of DMS by CH_3I. The resulting EMD is indicated by the vertical short thin dash line at 1.4 km.

As shown in Table 1, our estimated "h" values ranged from 0.5 to 0.9 km, giving an overall ensemble average of 0.7 km. EMD upper-limit values (based on CH_3I) varied from 1.0 to 1.8 km with the average being 1.4 km. The latter value suggests that on average the BL contained ~ 50% of the total DMS mass emitted from the ocean. For four of these EMD values, problems resulting from BuL biomass pollution or the total absence of CH_3I data led to our assigning the average EMD value to these runs. Based on the range of values estimated from those cases where upper limit EMD values could be more rigorously calculated, it appears that this assumption introduces no more than an additional 30% uncertainty in the DMS flux estimates for these runs.

4. Results and Discussion

4.1. DMS Fluxes

As discussed in section 3, the current analysis has been limited to evaluating only the upper and lower limits of the DMS flux. For all these cases the mid-value of the two limits defines our "best estimate" for the DMS flux for each sampling run. These mid-values for the 13 runs are given in Table 2 and are seen ranging from a low of 0.6 to a high of 3.0 μmol m^{-2} d^{-1} for PEM-A (September-October 1992) and from 1.4 to 1.9 μmol m^{-2} d^{-1} for PEM-B (February-March, 1994). These mid-values are shown binned as a function of latitude in Figure 3. The general trend for PEM-A is that of an increasing flux with increasing latitude; however, the number of observations cannot be considered statistically robust.

A detailed examination of the oxidation pathways most responsible for controlling the loss of DMS at each sampling location revealed that OH typically was responsible for 73% of the total, with NO_3 making up the remaining ~ 27%. Looking only at the six sampling cases (PWA-08, PWA-09, PWA-16, PWB-07, PWB-08, and PWB-09) having the highest NO_x levels, the average NO_3 contribution was found to increase to 40%. The maximum rate for NO_3/DMS oxidation was found for flights PWB-07 and PWB-08; here the rate for NO_3 slightly exceeded that for OH. Removing these two PEM-B fights dropped the NO_3 oxidation effect on the remaining 11 runs (e.g., PEM-A only) to just under 22%.

Table 1. Summary of Model Input Conditions

Flight Number	Sampling Time (local)	Latitude °N	Longitude °E	T[a] °C	Td[a] °C	$[O_3]$[a] ppbv	[CO][a] ppbv	[NO][a] pptv	$[NO_x]$[b] pptv	BL h km	EMD*[c] km	[DMS][a] pptv
PWA-06	17:13	28.0	146.7	25.2	21.4	10	68	3	11	0.6	1.1	34
PWA-08	15:56	28.7	147.0	25.0	21.9	21	91	3	19	0.9	1.4[d]	60
PWA-09	12:02	27.2	136.0	26.7	22.4	12	68	7	21	0.6	1.2	92
PWA-10	14:44	20.4	127.1	26.2	23.0	11	70	2	7	0.4	1.0	57
PWA-14	16:18	17.4	129.6	26.5	22.4	38	120	2	9	0.8	1.8	31
PWA-15	14:38	0.4	160.3	26.4	21.3	9	68	3	9	0.6	1.6	50
PWA-16	12:58	4.6	126.2	26.3	20.9	9	92	8	21	0.7	1.4[d]	26
PWA-18	12:36	13.0	159.8	25.1	22.0	8	73	2	6	0.6	1.4[d]	33
PWA-20	04:52	19.6	-155.2	21.1	18.9	22	76	1	5	0.7	1.3	22
PWA-20	08:26	19.6	-155.1	21.1	18.9	22	76	1	5	0.7	1.4[e]	22
PWB-07	15:57	13.6	147.0	24.9	17.8	26	100	5	17	0.7	1.4	19
PWB-08	15:10	16.4	145.9	23.4	17.9	27	121	5	19	0.9	1.5	13
PWB-09	15:12	1.0	146.5	25.1	20.6	19	98	6	18	0.7	1.6	27

PWA denotes PEM-West A and PWB denotes PEM-West B.

(a) Median observations.

(b) Model calculated quantity.

(c) EMD* = EMD upper limit estimated from CH_3I vertical profile.

(d) Buffer layer CH_3I influenced by pollution, average EMD* used.

(e) No CH_3I data available, average EMD used.

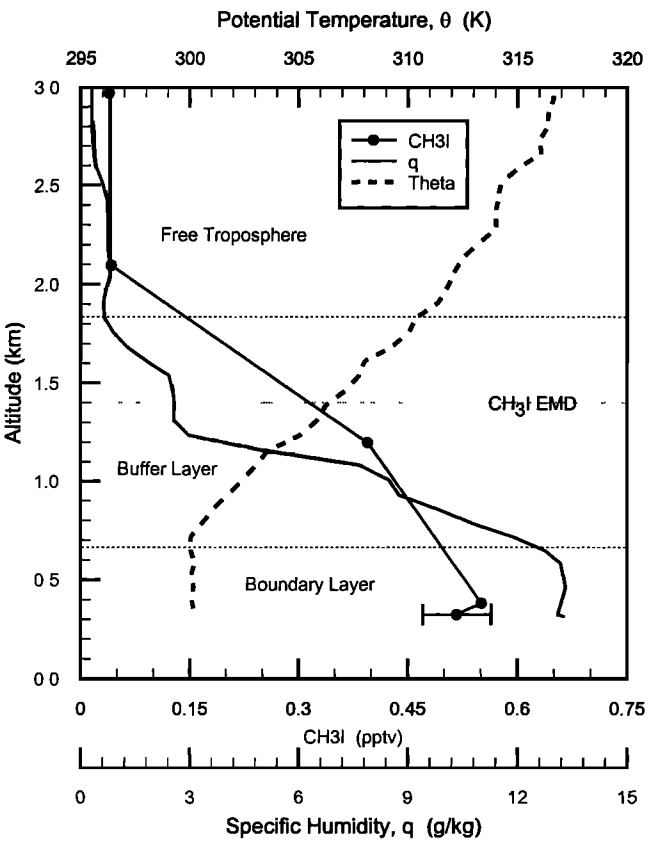

Figure 2. Vertical profiles of potential temperature (θ), specific humidity (q), and CH_3I for PEM-West B flight 7. The solid line denotes specific humidity; dashed line denotes potential temperature; and solid line with solid circle denotes CH_3I. Also shown here are the estimated BL height, BuL height (vertical long thin dash lines), and CH_3I EMD (vertical short thin dash line).

These results show that the NO_3/DMS reaction is typically of secondary importance as an oxidation agent for DMS. However, exclusion of this process for certain environments (e.g., high NO_x environment) could lead to a significant error. For example, under low OH and high NO_x conditions, it could dominate the oxidation processes. In the case of *Ayers et al.* [1995], the calculated austral winter flux estimates may have been as much as a factor of 2 or more higher if they had included the NO_3 reaction.

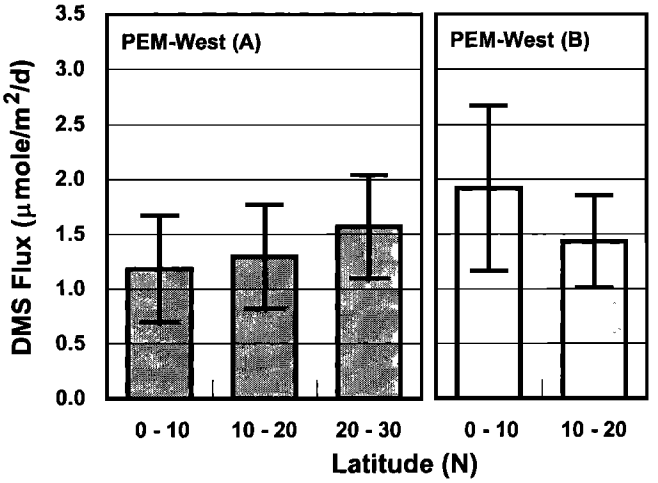

Figure 3. Latitudinal DMS flux distribution for PEM-West A and B. Data were average into 10° latitudinal bins. Solid bars indicate our best estimate of the DMS flux, while the error bars denote the upper and lower limits of these estimates.

Another issue related to the DMS oxidation was the significance of aqueous phase DMS oxidation by O_3 as suggested by *Lee and Zhou* [1994]. Here, we compare the magnitude of the potential impact of in-cloud oxidation of DMS with that of the gas phase oxidation. Assuming a liquid water content of 0.2 g/kg for typical marine stratocumulus clouds [*Wang and Albrecht,* 1994], the estimated DMS lifetime from the aqueous phase oxidation by O_3 would be nearly 40 days for the conditions encountered during PEM-West A and B sampling. On the other hand, the estimated DMS photochemical lifetime ranged from 1 to 2 days with an average of 1.2 days. Thus, even for the marine stratocumulus cloud conditions, the aqueous phase DMS oxidation would be less than 5% of that equivalent to the gas phase oxidation.

A comparison of the flux estimates given in Figure 3 with those reported by *Bates et al.* [1987], *Erickson et al.* [1990], and *Chin et al.* [1996] using sea-water DMS measurements is shown in Table 3. In this case all data have been grouped into latitudinal bins of 0-10°N, 10-20°N, and 20-30°N. From here it can be seen that for PEM-A our values lie within a factor of 2 of those reported by *Chin et al.* [1996], while significant disagreement (i.e., a factors of 3-5) is evident in the comparison with *Bates et al.* [1987] and *Erickson et al.* [1990]. Considering the limited PEM database being used in this

Table 2. Summary of Estimated DMS Flux

Flight[a] Number	Latitude °N	Longitude °E	Min F_{DMS} μmole/m²/d	Max F_{DMS} μmole/m²/d	Mid-value F_{DMS} μmole/m²/d
PWA-06	28.0	146 7	0 5	0 9	0.7
PWA-08	28.7	147.0	1 9	2 9	2.4
PWA-09	27.2	136.0	1 4	2.9	2.2
PWA-10	20.4	127.1	0 6	1.4	1.0
PWA-14	17.4	129 6	1 8	4.1	3.0
PWA-15	0.4	160 3	0 9	2 3	1.6
PWA-16	4.6	126.2	0 5	1.1	0.8
PWA-18	13.0	159 8	0 4	0 9	0 6
PWA-20	19.6	-155.2	0 5	1 0	0.8
PWA-20	19.6	-155.1	0 5	1.0	0.8
PWB-07	13.6	147.0	1 0	2.0	1.5
PWB-08	16.4	145.9	1 0	1.7	1.4
PWB-09	1.0	146 5	1.2	2.7	1 9

(a) PWA denotes PEM-West A and PWB denotes PEM-West B.

Table 3. Comparison with Literature Cited Oceanic DMS Flux Estimates

Latitude	This Work μmole/m²/d	*Bates et al.* 1987 μmole/m²/d	*Erickson et al.* 1990 μmole/m²/d	*Chin et al.* 1996 μmole/m²/d
0° - 10° N	1.2	3.3	3.0	1.9
10° - 20° N	1.3	4.6	4.4	1.0
20° - 30° N	1.6	3.6	5.1	1.4

comparison, one could argue that this level of disagreement is not that unreasonable.

A more realistic comparison of the two approaches has come recently in the airborne/ship study, The First Aerosol Characterization Experiment (ACE 1). Three flights were scheduled for intercomparison activity between the National Center for Atmospheric Research C-130 aircraft and the National Oceanic and Atmospheric Administration ship *Discovery* [*Bates et al.*, 1998]. Preliminary results from this comparison [*Davis et al.*, 1997] have shown that the difference in flux estimates ranged from a factor of 1.2 to 2.3, with an average value of 1.7, when the ship values were based on the piston velocity parameterization of *Liss and Merlivat* [1986]. If the piston velocity of *Wanninkhof* [1992] is used, this difference increased to 1.4-4.5 with an average of 2.5, the mass-balance/photochemical-modeling approach again giving the smaller value. Although further analysis of this common geographical data set is still ongoing, it does suggest that the mismatch in spatial and temporal scales between the PEM observations and the database used in the GCM modeling studies could be responsible for some significant fraction of the difference cited above.

4.2. Sensitivity Analysis

Recall, earlier we briefly addressed the issue of uncertainties associated with the basic input parameters to (4). These include EMD, $[DMS]_{OBS}$, OH, and NO_3. To better quantify the impact from these uncertainties, we have here carried out several sensitivity runs in which the magnitudes of these critical variables were varied by factors of ± 2. These tests were performed on all 13 runs included in the current analysis. The resulting average shift in the calculated DMS fluxes are summarized in Table 4. From here it can be seen that for the parameters OH, EMD, and $[DMS]_{OBS}$ a near linear relationship is seen between the DMS flux and the shift in the value of the parameter. Not surprisingly, the average effect due to a change in $[NO_3]$ is seen as only 10-20%.

A propagation of error analysis against the first three factors has shown that the overall uncertainty in our flux estimates is in the range of 31-51%, the average being 41%. In this analysis we assigned an uncertainty to OH of ± 25% [*D. D. Davis et al.*, 1993; *Crawford*, 1997; *Jefferson et al.*, 1998; *Mauldin et al.*, 1998a; *R. L. Mauldin, et al.*, Measurements During PEM Tropics: Observations and Model Comparisons, submitted to Journal of Geophysical Research, 1998b; *Davis et al.*, 1998b]. In assigning the OH uncertainty, one of the factors considered was the possible error associated with the difference in the rate of OH oxidation of DMS in the BL versus the BuL. However, model simulations showed that this difference was typically ≤ 20%. For EMD, we assumed that the value of the standard deviation was half of the difference between the value based on BL height and that derived from CH_3I, for example, see Table 1. The finally variable, $[DMS]_{OBS}$, was assigned an uncertainty given by Drexel investigators, i.e., ± 2 pptv [*Thornton et al.*, 1996; *Hoell et al.*, 1996]. Overall, the uncertainty in the photochemical approach (e.g., 41%) appears to compare very favorably with other methods.

Table 4. Summary of Sensitivity Calculation

Variables	Change Factor[a]	Change Factor in F_{DMS}
EMD	± 2	± 2.0
$[DMS]_{obs}$	± 2	± 1.8
OH	± 2	± 1.8
NO_3	± 2	± 1.2

(a) Here denotes the multiplicative factor (+) and dividing factor (-), respectively.

(b) The values reported here are the averages from calculations for all PEM-West A and PEM-West B runs.

Although the above error assessment (based on known sources of error) suggest that for a given time and place the probable error would fall between a factor of 1.3 and 1.5, the latter analysis does not consider other biases that might lie hidden in the data and not be easily quantified. These include any bias introduced into the analysis from our having to use DMS data from single event sampling (e.g., 30-45 min) rather than having the more ideal 24-hour continuous DMS data (e.g., see section 4.2.1 for details). Even more serious could be the potential bias introduced by stochastic events. The most significant of these we now believe would involve major solar flux variations 24-48 hours prior to the time of sampling. This possibility is explored in greater detail in section 4.2.2.

4.2.1. Point versus continuous data. Simulations designed to evaluate the error resulting from the use of snapshot (e.g., 30-45 min) aircraft data, rather than near continuous monitoring, were performed using the earlier gas phase DMS databases reported by *Bandy et al.* [1996] as well as those by *Gregory et al.* [1993]. To begin this assessment, a comparison was first carried out to determine how closely the photochemical approach would agree with a nonphotochemical approach with both approaches using continuous data. This exercise involved the use of *Bandy et al.'s* [1996] recorded in a ground-based sampling study at Christmas Island in the central equatorial Pacific. This atmospheric sulfur experiment, conducted during the summer of 1994, encompassed continuous recordings (5-10 min time resolution) of gas phase DMS and SO_2 over a period of several days. The BL height was estimated during this field study from local soundings. Also recorded were measurements for a limited number of photochemical parameters. Included in this list were O_3 and UV irradiance. From these near continuous DMS data, Bandy et al. used a simple comparison of the nighttime and daytime levels of DMS in conjunction with BL height information to deduce a DMS flux of 5.3 μmol m^{-2} d^{-1}. Taking this same data set, we used the mass-balance/photochemical modeling approach described in this work to generate the results shown in Figure 4. From this analysis the photochemically derived DMS flux is seen as lying within 10% of that estimated by Bandy et al. Also quite evident from Figure 4, the model predicted DMS profile is seen to agree extremely well with the

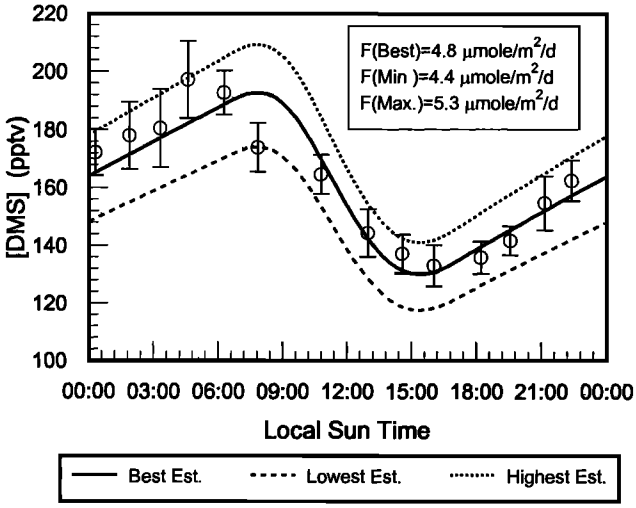

Figure 4. Test of single point sampling versus continuous sampling. Solid squares denote DMS hourly average over a 5-day period. Error bars indicate the atmospheric variability in DMS. Curves represent model simulated DMS values. Top and bottom curves correspond to the maximum and minimum flux estimates derived from using a single data point; whereas, the middle curve represents the "best estimate" of the DMS flux.

DMS observations (i.e., 15%). Thus this result can be viewed as validating the mass-balance/photochemical-flux approach, at least under the conditions of the Christmas Island experiment.

The above results suggest that the photochemical approach can be used to provide reasonable DMS sea-to-air flux estimates under tropical conditions, given that a complete diel DMS profile is available and that some reasonable information exists concerning the BL height and atmospheric mixing. As noted in section 3, during PEM-A and -B, only snapshot data segments were available. Thus, this aircraft snapshot data represents only one point in the profile shown in Figure 4. The question may be asked, then, whether the more limited airborne sampling scenario can really be used to accurately evaluate DMS fluxes. To address this question, we carried out a new flux assessment of the Christmas Island data in which only a single data point from the 24-hour profile of *Bandy et al.* [1996] was used. This resulted in the generation of minimum and maximum DMS profiles from which a range of flux estimates could be derived as shown in Figure 4. In this case, the results clearly indicate that the bias generated in these simulations is 11% of the "best estimate," the latter value being the product of the entire diel DMS profile.

Using the airborne DMS database generated during NASA's GTE CITE-3 (Chemical Instrumentation Test and Evaluation) [*Gregory et al.*, 1993], a second level of testing of the "continuous" versus "point" data sampling problem was also carried out. What makes the latter airborne data set unique is that it involved extensive BL sampling runs, typically 3-4 hours in duration. Like the Christmas Island data, these data were also generated in the tropics but with the geographical location being the tropical South Atlantic Ocean. The sampling strategy in CITE-3 also involved flights that covered both the early morning maximum and afternoon minimum in DMS levels. Thus the CITE-3 database bracketed the most critical times of the DMS diel cycle. Our test simulations involved comparing flux estimates based on a single hour of data with that calculated using the entire sampling period. These results were also quite encouraging. For example, the difference between the two simulations was less than 25%. These results, as well as those discussed above using the Christmas Island data, lead to the conclusion that the use of airborne snapshot DMS data, as collected during PEM-A and -B, should not have introduced more than a 25% error into our final DMS flux estimates.

4.2.2. Stochastic events. As noted earlier in this text, the DMS sea-to-air flux estimates using the photochemical approach are also potentially subject to a bias whose source can originate outside of the temporal sampling window. For example, if major fluctuations were to occur in the solar flux 24 hours in advance to the sampling, the observed atmospheric DMS level is unlikely to be at quasi-steady-state. A simple definition for the quasi-steady-state configuration as related to DMS is that the diel change in DMS, in magnitude and in trend, would reproduce itself each day. For this condition to be realized for DMS, all other related variables would necessarily also have to be at quasi-steady- state. This includes both OH and NO_3. In addition, the values of EMD and the DMS sea-to-air flux itself would need to be relatively constant. Any stochastic change that influenced one of these parameters would cause atmospheric levels of DMS to deviate from the original quasi-steady-state value. If this perturbation were then suddenly removed, DMS values would be expected to gradually return to the original quasi-steady-state configuration. Alternatively, if the perturbation were to be permanent in nature, DMS would eventually reach a new quasi-steady-state reflecting the new condition. Typically, two-three photochemical lifetimes are required for the DMS to return to the quasi-steady-state condition. Thus, to the extent that DMS sampling were to occur reasonably soon after a stochastic perturbation, the observed DMS would not be representative of the original quasi-steady-state value. This means that any DMS flux estimate based on this observation would necessarily be biased. The magnitude of the bias would be a function of the difference between the observed DMS value and the value that would eventually be seen for that time of day when the new quasi- steady-state condition set up. As noted above, this type of error is especially acute in the case of airborne sampling since only "snapshots" of the time history are recorded. In the text that follows we explore the impact of what we believe would be the most common of the stochastic events, namely, variations in OH due to abrupt shifts in BL cloud coverage.

In the test case, the sampling region was assumed to have both a uniform DMS flux field and a constant EMD of 1.0 km throughout the test period. The DMS flux was taken to be 2.5 μmol m^{-2} d^{-1}. The stochastic event was one that involved an abrupt change in cloud coverage and thus produced a sudden change in OH levels. The approach taken involved first initializing the model such that a quasi-steady-state was reached in the OH profile (the diel average of which was 1.5 $\times 10^6$ molecule cm^{-3}); then, for 4 hours, from 1000-1400 UT, a systematic decrease of 50% in the OH level was introduced, reflecting a major reduction in the solar irradiance. Finally, the OH profile was returned to its original quasi-steady-state value following the 4-hour perturbation. DMS samples were assumed to be taken during the time of perturbation and at times corresponding to 2, 8, 16, 32, and 64 hours following

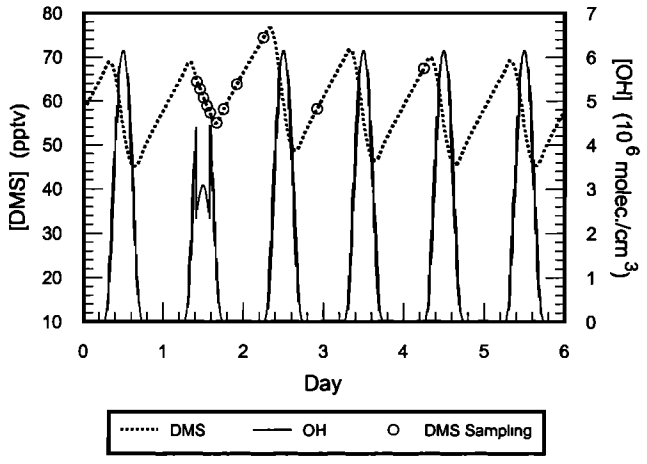

Figure 5. Effect of solar/OH perturbations on DMS concentration profile. Dashed line indicates OH profile with the solar perturbation occurring in day 2. Solid line indicates model simulated DMS levels resulting from the OH perturbation. Open squares indicate an assumed sampling scenario used to derive the magnitude of bias in the model calculated DMS flux.

the perturbation. The results from this simulation are shown in Figure 5. From here it can be seen that the perturbation produces both a new elevated "minimum" in DMS during the late afternoon as well as a new elevated "maximum" the following morning. The impact upon the estimated DMS flux is shown in Figure 6. These results indicate that if one were to calculate the "true" DMS flux (i.e., what would be estimated from OH and DMS if sampled before the perturbation), it would be higher than that estimated during the perturbation (if the latter were the only data sampled) by a factor of nearly 1.4. However, if sampling occurred only after the 4-hour perturbation, the "true" flux would tend to be lower than the estimated flux by a factor of ~1.2. This bias would rapidly decrease to < 10% for times greater than one photochemical lifetime. However, the longer the perturbation time period preceding the actual sampling, the larger would be the bias appearing in the estimated flux.

Similar tests were also performed to examine the magnitude of error introduced from sudden changes in EMD and F_{DMS}. In this case our simulations showed that a sudden change of factor of 1.5 (highly unlikely) in EMD (or F_{DMS}) would cause a deviation in the flux estimate by nearly a factor of 1.5, if sampling were to occur during the time period of the perturbation. However, the magnitude of this bias decreases rapidly with elapsed time after the perturbation, like in the previous case. After one photochemical lifetime, the bias decreased to only about 15%. As stated before, the magnitude of this type of bias is strongly dependent on the magnitude of the perturbation itself.

4.2.3. Influence of large-scale atmospheric subsidence or convergence. Another potential source of error in our flux assessment is that resulting from mesoscale subsidence or convergence. For example, large scale subsidence would represent a loss of DMS due to dilution of the BuL and BL by free troposphere (FT) air depleted in DMS. In our earlier presentation of the mass-balance equation, we assumed that the mean vertical velocity "w" was zero. Inclusion of large-scale subsidence or convergences processes lead to a modification of the basic DMS mass-balance equation as shown in (5):

$$\frac{d[DMS]}{dt} = \frac{F_{s-a}}{EMD} - \left(k_{OH}[OH] + k_{NO_3}[NO_3]\right)[DMS] + \frac{1}{EMD}\int_0^{h_{BuL}} W\left(\frac{\partial[DMS]}{\partial z}\right)dz \quad (5)$$

This form of the equation assumes a negligible horizontal DMS gradient with the quantities "w" and ∂[DMS]/∂z representing the mean vertical velocity and the DMS vertical gradient, respectively. To evaluate (5), values of "w" can be assessed as a function of altitude from model assimilated global meteorological databases such as European Centre for Medium-Range Weather Forecasts (ECMWF) or National Centers for Environmental Predication (NCEP). Even so, it must be recognized that these values inherently have large uncertainties associated with them since they are calculated by taking the difference between two large quantities, namely the horizontal wind divergence in the "x" and "y" wind fields. One is therefore inclined to conclude that such daily generated "w" values may not be as reliable as those derived from averaging values taken over a period of a month, as are reported as part of the NCEP data products.

The DMS vertical gradient, ∂[DMS]/∂z, can typically be estimated directly from airborne DMS vertical data; but temporal variations in "w" as well as ∂[DMS]/∂z are usually not available. Thus, as a first-order approximation, we have here assumed that these variations are negligibly small. For this special case, the potential bias in the DMS flux due to large-scale mean vertical motion can be evaluated from (6):

$$\Delta F = \int_0^{h_{BuL}} w\frac{\partial[DMS]}{\partial z}dz \quad (6)$$

In the evaluation of (6), it is recognized that the BL is typically well mixed. This means that the magnitude of the DMS vertical gradient for this regime is negligibly small, and therefore the influence of large-scale vertical motion tends to be confined to the BuL region. Equation (6) can therefore be rewritten as

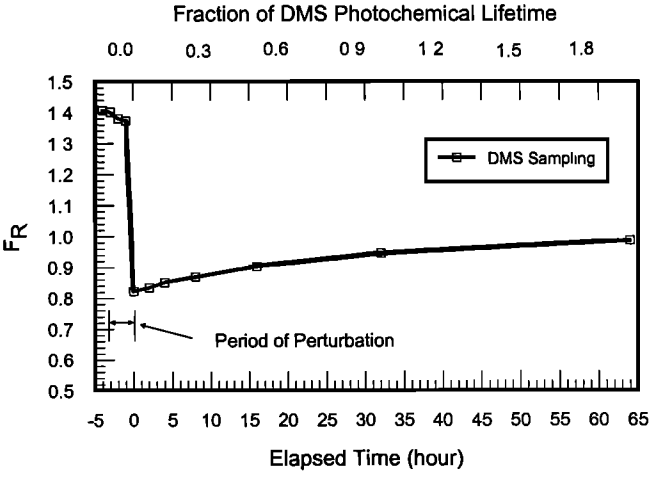

Figure 6. F_R versus elapse time following solar/OH perturbation. F_R is defined as the ratio of the "true" DMS flux (estimated from data sampled before the perturbation) to the flux estimate derived from OH and DMS data recorded during and after the perturbation.

$$\Delta F = \int_{h_{BL}}^{h_{BuL}} w \frac{\partial [DMS]}{\partial z} dz \qquad (7)$$

In (7), ∂[DMS]/∂z is always negative, reflecting its oceanic origin. As noted above, this means that without the inclusion of large-scale subsidence our earlier estimated DMS flux values would be underestimated. However, the presence of weak convergence would lead to an overestimate. (The authors note that for the special case of strong convergence we would also overestimate the flux; however, there are still other complications involved in the analysis of this scenario that render it impractical to treat.)

As a sensitivity test, we have explored the possible magnitude of the bias resulting from (7) for a midlatitude marine setting in which all necessary parameters were available for evaluating this equation. This midlatitude case involved data recorded during the airborne field study ACE 1. During flight 24 of this study, it was documented that most of the low-altitude sampling was significantly influenced by large-scale subsidence in the region. The average BuL mean vertical velocity and DMS vertical gradient were estimated at -0.24 cms^{-1} [*Wang et al.*, 1999] and 100 pptv km^{-1}, respectively. The vertical velocity was calculated from ECMWF data, while the DMS gradient was derived from direct observations within the BuL. Integration of (7) resulted in a bias of 0.6 μmol m^{-2} d^{-1} or about 25% of the flux estimated without considering subsidence.

During PEM-West A and B, the BuL DMS database was inadequate for purposes of establishing a reliable DMS vertical gradient, thus, making it impossible to evaluate the potential bias for each PEM-West A and B flux determination. What was done in lieu of this full quantitative assessment was to examine the monthly mean vertical velocity for each of the PEM-West A and B cases reported on in this work. This analysis (based on NCEP data) indicated that about half of the cases studied were influenced by subsidence, while the other half was affected by weak convergence. In all cases but one, however, the magnitude of the BuL mean vertical velocity was quite small, typically < 0.15 cms^{-1}. For one isolated case, PWA-16, the value of "w" approached 0.5 cms^{-1}. This suggests that our first-order approximation assessment of DMS fluxes during PEM-West A and B was only slightly influenced by large-scale atmospheric subsidence or convergence. Given the mean "w" values taken from the NCEP data, we would place this error at somewhere between 0 and 30%. Even for run PWA-16, the bias is unlikely to have exceeded 45%.

5. Summary and Conclusions

This study has evaluated the DMS sea-to-air flux in the western North Pacific using a mass-balance/photochemical-modeling approach. It used as its database measurements of DMS and photochemical variables recorded during NASA's GTE PEM-A and -B programs. These airborne campaigns occurred in the fall of 1991 and winter/earlier spring of 1994, respectively. The results indicate that the DMS flux ranged from 0.6 to 3.0 μmol m^{-2} d^{-1} during the fall and 1.4 to 1.9 μmol m^{-2} d^{-1} during the winter campaign, with the latter flux range clearly a reflection of the limited number of sample runs (e.g., 3). These estimates were generally compatible with the results from GCM-type studies; however, because of differences in temporal and geographical spatial coverage, no quantitative comparison was possible.

Simulations in which "snapshot" type DMS data were compared with near continuous data demonstrated that airborne sampling of the type carried out in PEM-A and -B can be used to evaluate reliable values of the DMS flux. A key factor here is that the DMS must be predominantly removed by local photochemical processes; thus DMS lifetimes must be relatively short, i.e., $\leq$ 2.5 days. Sensitivity tests, in fact, showed that the key factors controlling the flux estimate were the levels of OH, equivalent mixing depth, and the observed level of DMS. The propagated error for this approach was estimated at between 31-51% when evaluated in terms of a specific time and sampling location. Systematic errors were also explored. These were identified in two forms: (1) the neglect of large-scale vertical motion and (2) the impact from stochastic events involving cloud coverage. We have estimated the magnitude of the first source of error to be in the range of 0-30%; whereas, sensitivity analysis suggest that the second could be as large as a factor of 2. The latter value was arrived at from our examination of specific types of stochastic events and how these events might impact upon the photochemical flux estimate. In these simulations it was shown that when atmospheric DMS is not in quasi-steady-state the estimated flux will be biased. Under conditions involving "snapshot" airborne sampling, DMS levels were found to be quite sensitive to solar shifts that produced significant changes in the diel OH field. It was concluded that stochastic changes of this type are quite likely the single most important factor that would dictate the accuracy of photochemically derived DMS fluxes when using airborne "snapshot" sampling. Thus improvements in the accuracy of this approach involve having a more detailed meteorological analysis during the 24 hours preceding the sampling window as well as having high-resolution DMS measurements, real-time measurements of OH, and a larger airborne sampling window. Still, a final uncertainty in this approach involves the role of atmospheric mixing, particularly that involving convective events. In such cases, high-resolution vertical DMS data would be especially important.

Overall, we can conclude that the mass-balance/photochemical approach is a very promising one for evaluating sea-to-air DMS fluxes. It has the potential to greatly augment the existing DMS flux database and to also possibly provide important insights into the evaluation of the marine "piston velocity."

Acknowledgments. This work was supported in part by funds from the National Aeronautics and Space Administration under grants NCC-1-148, NCC-1438, and NAGW-4908 (formerly NAGW-3770). The authors would like to express their deep appreciation to Don Lenschow of NCAR and Qing Wang of Naval Postgraduate School for insightful discussions. D. D. Davis would also like to thank the project office at NASA Langley Research Center and the flight crews at NASA Ames Research Center for their dedicated support of the PEM-West A and B programs.

References

Andreae, M. O., and H. Raemdonck, Dimethyl sulfide in the ocean and the marine atmosphere: A global view, *Science*, *221*, 744-747, 1983.

Ayers, G. P., S. T. Bentley, J. P. Ivy, and B. W. Forgan, Dimethylsulfide in marine air at Cape Grim, 41°S, *J. Geophys. Res.*, *100*, 21,013-21,021, 1995.

Bandy, A. R., D. C. Thornton, and A. R. Driedger III, Airborne measurements of sulfur dioxide, dimethyl sulfide, carbon disulfide, and carbonyl sulfide by isotope dilution gas chromatography/mass spectrometry, *J. Geophys. Res.*, *98*, 23,423-23,433, 1993.

Bandy, A. R., D. C. Thornton, B. W. Blomquist, S. Chen, T. P. Wade, J. C. Ianni, G. M. Mitchell, and W. Nadler, Chemistry of dimethyl sulfide in the equatorial Pacific atmosphere, *Geophys. Res. Lett.*, *23*, 741-744, 1996.

Barnard, W. R., M. O. Andreae, W. E. Watkins, H. Bingemer, and H.-W. Georgii, The flux of dimethyl sulfide from the oceans to the atmosphere, *J. Geophys. Res.*, *87*, 8787-8793, 1982.

Barnes, I., V. Bastain, K. H. Becker, and D. Martin, Fourier transform IR studies of the reactions of dimethyl sulfoxide with OH, NO_3, and Cl radicals in *Biogenic Sulfur in the Environment*, edited by E. S. Saltzman and W. J. Cooper, *American Chemical Society Press*, Washington, D.C., 1989.

Barnes, I., K. H. Becker, and N. Mihalopoulos, FTIR product study of the photolysis of CH_3SSCH_3: Reactions of the CH_3 radical in *Dimethylsulfoxide: Ocean, Atmosphere and Climate*, edited by G. Restelli and G. Angeletti, Academic, San Diego, California. pp. 197-210, 1993.

Barnes, I., K. H. Becker, and I. Patroescu, The tropospheric oxidation of dimethyl sulfide: A new source of carbonyl sulfide, *Geophys. Res. Lett.*, *21*, 2389-2392, 1994.

Bates, T. S., J. D. Cline, R. H. Gammon, and S. R. Kelly-Hansen, Regional and seasonal variations in the flux of oceanic dimethyl sulfide to the atmosphere, *J. Geophys. Res.*, *92*, 2930-2938, 1987.

Bates, T. S., B. K. Lamb, A. Guenther, J. Dignon, and R. E. Stoiber, Sulfur emissions to the atmosphere from natural sources, *J. Atmos. Chem.*, *14*, 315-337, 1992.

Bates, T. S., B. J. Huebert, J. L. Gras, F. B. Griffths, and P. A. Durkee, International Global Atmospheric Chemistry (IGAC) Project's First Aerosol Characterization Experiment (ACE 1): Overview, *J. Geophys. Res.*, *103*, 16,297-16,318, 1998

Berresheim, H., P. H. Wine, and D. D. Davis, Sulfur in the atmosphere, in *Composition, Chemistry, and Climate of the Atmosphere*, edited by H. B. Singh, pp. 251-307, Van Nostrand Reinhold, New York, 1995.

Chameides, W. L., et al., Observed and model-calculated NO_2/NO ratios in tropospheric air sampled during the NASA GTE/CITE 2 field study, *J. Geophys. Res.*, *95*, 10,235-10,247, 1990.

Chen, G., A study of tropospheric photochemistry in the subtropical/tropical North and South Atlantic, *Ph.D. dissertation*, Georgia Inst. of Tech., Atlanta, 1995.

Chin, M., D. J. Jacob, G. M. Gardner, M. S. Foreman-Fowler, and P. A. Spiro, A global three-dimensional model of tropospheric sulfate, *J. Geophys. Res.*, *101*, 18,667-18,690, 1996.

Crawford, J. H., et al, Implications of large scale shifts in tropospheric NO_x levels in the remote tropical Pacific, *J. Geophys. Res.*, *102* 28,447-28,468, 1997.

Crawford, J. H., et al., An assessment of ozone photochemistry in the extratropical western North Pacific: Impact of continental outflow during the late winter/earlier spring, *J. Geophys. Res.*, in press, 1998.

Dacey, J. W., and S. G. Wakeham, Oceanic dimethyl sulfide: Production during zooplankton grazing on phytoplankton, *Science*, *233*, 1314-1316, 1986.

Davis, D. D., J. D. Bradshaw, M. O. Rodgers, S. T. Sandholm, and S. KeSheng, Free tropospheric and boundary layer measurements of NO over the central and eastern North Pacific Ocean, *J. Geophys. Res.*, *92*, 2049-2070, 1987.

Davis, D. D., J. Hoell, G. Gregory, and R. Bendura, Operational overview of NASA GTE/CITE-3 Airborne Experiment (Abstract), EOS Trans. AGU *71*, 1254, 1990.

Davis, D. D., et al., Photostationary state analysis of the NO_2-NO system based on airborne observations from the subtropical/tropical North and South Atlantic, *J. Geophys. Res.*, *98*, 23,501-23,523, 1993.

Davis, D. D., et al., Assessment of ozone photochemistry in the western North Pacific as inferred from PEM-West A observations during the fall 1991, *J. Geophys. Res.*, *101*, 2111-2134, 1996a.

Davis, D. D., J. H. Crawford, S. Liu, S. McKeen, A. Bandy, D. Thornton, F. Rowland, and D. Blake, Potential impact of iodine on tropospheric levels of ozone and other critical oxidizing species, *J. Geophys. Res.*, *101*, 2135-2147, 1996b.

Davis, D. D., Z. Shon, G. Chen, B. J. DiNunno, A. R. Bandy, and D. C. Thornton, Photochemical assessment of DMS flux over the Southern Ocean as inferred from ACE-1 Observation, EOS Trans. AGU, *78 (46)*, Fall Meet. Suppl., F122, 1997.

Davis, D. D., G. Chen, P. Kasibhatla, H. Berresheim, F. L. Eisele, D. Tanner, and A. Jefferson, DMS oxidation in the Antarctic marine boundary layer: Comparison of model simulations with observations for DMSO(g), $DMSO_2$(g), MSA(g), and H_2SO_4(g), *J. Geophys. Res.*, *103*, 1657-1746, 1998a.

Davis, D. D., G. Chen, F. Eisele, B. Huebert, D. Tanner, L. Mauldin, A. Bandy, D. Thornton, and D. Lenschow, DMS oxidation in the equatorial Pacific: Comparison of model simulations with field observations for DMS, SO_2, H_2SO_4(g), SMA(g), MS, and NSS, *J. Geophys. Res.*, in press, 1998b.

Davis, H. F., B. Kim, H. S. Johnston, and Y. T. Lee, Dissociation energy and photochemistry of NO_3, *J. Phys. Chem*, *97*, 2172-2180, 1993.

Davison, B., and C. N. Hewitt, Natural sulfur species from the North Atlantic and their contribution to the United Kingdom sulfur budget, *J. Geophys. Res.*, *97*, 2475-2488, 1992.

Erickson, D. J., III, S. J. Ghan, and J. E. Penner, Global ocean-to-atmosphere dimethyl sulfide flux., *J. Geophys Res.*, *95*, 7543-7552, 1990.

Gregory, G. L., L. S. Warren, D. D. Davis, M. O. Andreae, A. R. Bandy, R. J. Ferek, J. E. Johnson, E. S. Saltzman, and D. J. Cooper, An intercomparison of instrumentation for tropospheric measurements of dimethyl sulfide: Aircraft results for concentrations at the parts-per-trillion level, *J. Geophys Res.*, *98*, 23,373-23,388, 1993.

Hesstvedt, E., Ø. Hov, and I. S. A. Isaksen, Quasi-steady-state approximations in air pollution modeling: A comparison of two numerical schemes for oxidant prediction, *Int. J. Chem. Kinet.*, *10*, 971-994, 1978.

Hoell, J. M., D. D. Davis, S. C. Liu, R. Newell, M. Shipham, H. Akimoto, R. J. McNeal, R. J. Bendura, and J. W. Drewry, Pacific Exploratory Mission-West (PEM-West A): September-October 1991, *J. Geophys. Res.*, *101*, 1641-1653, 1996.

Hoell, J. M., et al., The Pacific Exploratory Mission-West Phase B: February-March 1994, *J. Geophys. Res. 102*, 28,223-28,239, 1997.

Hynes, A. J., P. H. Wine, and D. H. Semmes, Kinetics and mechanism of OH reactions with organic sulfides, *J. Phys. Chem.*, *90*, 4148-4156, 1986.

Intergovernmental Panel on Climate Change, *Climate Change 1995, The Science of Climate Change*, edited by J. T. Houghton et al., Cambridge Univ. Press, New York, 1995.

International Geosphere-Biosphere Programme, *A Study of Global Change, IGBP: A Plan for Action, Rep. 4*, 200 pp., Stockholm, Sweden, 1988.

International Global Atmospheric Chemistry (IGAC) Project, *The Operational Plan*, edited by A. A. P. Pszenny and R. G. Prinn, *Rep. 32*, 134 pp., Int. Geosphere-Biosphere Programme, Stockholm, Sweden, 1994.

Jefferson, A., D. J. Tanner, F. L. Eisele, D. D. Davis, G. Chen, J. Crawford, J. W. Huey, A. L. Torres, and H. Berresheim, OH photochemistry and methane sulfonic acid formation in the coastal Antarctic boundary layer, *J. Geophys. Res.*, *103*, 1647-1656, 1998.

Jodwalis, C. M., and R. L. Benner, Sulfur gas fluxes and horizontal inhomogeneities in the marine boundary layer, *J. Geophys. Res.*, *101*, 4393-4401, 1996.

Johnston, H. S., C. A. Cantrell, and J. G. Calvert, Unimolecular decomposition of NO_3 to form NO and O_2 and a review of N_2O_5/NO_3 kinetics, *J. Geophys. Res.*, *91*, 5159-5172, 1986.

Keller, M. D., W. K. Bellows, and R. R. L. Guillard, A survey of dimethyl sulfide production in 12 cases of marine phytoplankton, in *Biogenic Sulfur in the Environment*, edited by E. Saltzman and W. Cooper, pp. 167-182, Am. Chem. Soc., Washington, D.C., 1989.

Kreidenweis, S. M., and J. H. Seinfeld, Nucleation of sulfuric acid-water and methanesulfonic acid-water solution particles: Implications for the atmospheric chemistry of organosulfur species, *Atmos. Environ.*, *22*, 283-296, 1988.

Langner, J., and H. Rodhe, A global three-dimensional model of the tropospheric sulfur cycle, *J. Atmos. Chem.*, *13*, 225-263, 1991.

Lee, Yin-Nan and Xianliang Zhou, Aqueous reaction kinetics of ozone and dimethylsulfide and its atmospheric implications, *J. Geophys. Res.*, *99*, 3,597-3,605, 1994.

Lenschow, D. W., A proposal for measuring entrainment into the cloud-capped boundary layer, 29-55, paper presented at the ETL/CSU Cloud-Related Process Modeling and Measurement Workshop, Boulder, Colorado, October 23-25, 1995.

Lenschow, D. W., I. R. Paluch, A. R. Bandy, and D. C. Thornton, Use of a mixed-layer model to estimate dimethyl sulfide flux and

application to other trace gas species fluxes, J. Geophys. Res., in press, 1998.

Liss, P. S., and L. Merlivat, Air-sea gas exchange rates: Introduction and synthesis, in *The Role of Air-Sea Exchange in Geochemical Cycling,* edited by P. Buat-Ménard, pp. 113-127, D. Reidel, Norwell, Mass., 1986.

McFarland, M., D. Kley, J. W. Drummond, A. L. Schmeltekopf, and R. H. Winkler, Nitric oxide measurements in the equatorial Pacific region, *Geophys. Res. Lett., 6,* 605-608, 1979.

Merrill, J. T., R. E. Newell, and A. S. Bachmeier, A meteorological overview for the Pacific Exploratory Mission-West, Phase B, *J. Geophys. Res., 102,* 28,241-28,253, 1997.

Penner, J. E., C. A. Atherton, and T. Graedel, Global emissions and models of photochemically active compounds, in *Global Atmospheric-Biospheric Chemistry,* edited by R. G. Prinn, pp. 223-248, Plenum, New York, 1994.

Pham, M., J. F. Müller, G. Brasseur, C. Granier, and G. Megie, A three-dimensional study of the tropospheric sulfur cycle, *J. Geophys. Res., 100,* 26,061-26,092, 1995.

Putaud, J.-P., and B. C. Nguyen, Assessment of dimethylsulfide sea-air exchange rate, *J. Geophys. Res., 101,* 4403-4411, 1996.

Ridley, B. A., M. A. Carroll, and G. L. Gregory, Measurements of nitric oxide in the boundary layer and free-troposphere over the Pacific Ocean, *J. Geophys. Res., 92,* 2025-2047, 1987.

Russell, L. M., D. H. Lenschow, K. K. Laursen, T. S. Bates, A. R. Bandy, and D. Thornton, Bidirectional mixing in a marine PBL overlain by a second turbulent layer, *J. Geophys. Res., 103,* 16,411-16,432, 1998.

Saltzman, E. S., and W. J. Cooper, Dimethyl sulfide and hydrogen sulfide in marine air, in *Biogenic sulfur in the environment, ACS Symposium Series,* Vol. 393, pp. 330-351, Am. Chem. Soc., Washington, D.C., 1989.

Smethie, W. M., Jr., T. Takahashi, D. W. Chipman, and J. R. Ledwell, Gas exchange and CO_2 flux in the tropical Atlantic Ocean determined from ^{222}Rn and pCO_2 measurements, *J. Geophys. Res., 90,* 7005-7022, 1985.

Sørensen, S., H. Falbe-Hansen, M. Mangoni, J. Hjorth, and N. R. Jensen, Observation of DMSO and $CH_3S(O)OH$ from the gas phase reaction between DMS and OH, *J. Atmos. Chem., 24,* 299-315, 1996.

Spiro, P. A., D. J. Jacob, and J. A. Logan, Global inventory of sulfur emissions with 1°×1° resolution, *J. Geophys. Res., 97,* 6023-6036, 1992.

Stull, R. B., *An Introduction to Boundary Layer Meteorology,* Klüwer Acad., Norwell, Mass., 1988.

Thompson, A. M., W. E. Esaias, and R. L. Iverson, Two approaches to determining the sea-to-air flux of dimethyl sulfide-satellite ocean color and a photochemical model with atmospheric measurements, *J. Geophys. Res., 95,* 551-558, 1990.

Thompson, A. M., et al., Ozone observations and a model of marine boundary layer photochemistry during SAGA 3, *J. Geophys. Res., 98,* 16,955-16,968, 1993.

Thornton, D. C., A. R. Bandy, B. W. Blomquist, D. D. Davis, and R. W. Talbot, Sulfur dioxide as a source of condensation nuclei in the upper troposphere of the Pacific Ocean, *J. Geophys. Res., 101,* 1883-1890, 1996.

Wang, Q., and B. A. Albrecht, Observations of Cloud top Entrainment in Marine Stratocumulus Clouds, *J. Atmos. Sci., 51,* 1,530-1,547, 1994.

Wang, Q., K. Suhre, P. Krummel, S. Siems, L. Pan, T. Bates, J. E., Johnson, D. H. Lenschow, B. J. Heubert, G. L. Kok, R. D. Schillawski, A. S. H. Prevot, and S. Businger, Characteristics of the marine boundary layers during two lagrangian measurement periods, 1: General conditions and mean characteristics, *J. Geophys. Res.,* in press, 1999.

Wanninkhof, R., Relationship between wind speed and gas exchange over the ocean, *J. Geophys. Res., 97,* 7373-7382, 1992.

Wanninkhof, R., J. R. Ledwell, and W. S. Broecker, Gas exchange-wind speed relation measured with sulfur hexaflouride on a lake, *Science, 227,* 1224-1226, 1985.

Yvon, S. A., E. S. Saltzman, D. J. Cooper, T. S. Bates, and A. M. Thompson, Atmospheric sulfur cycling in the tropical Pacific marine boundary layer (12°S, 135°W): A comparison of field data and model results, 1, Dimethyl sulfide, *J. Geophys. Res., 101,* 6899-4909, 1996.

A. Bandy and D. Thornton, Department of Chemistry, Drexel University, Philadelphia, PA 19104.

D. Blake, Department of Chemistry, University of California, Irvine, CA 92697.

G. Chen and D. Davis, School of Earth and Atmospheric Sciences, Georgia Institute of Technology, Atlanta, GA 30332. (e-mail: gc37@prism.gatech.edu).

P. Kasibhatla, School of Environment, Duke University, Durham, NC 27706.

(Received July 29, 1997; revised September 24, 1998;
accepted September 25, 1998.)